Lithium Diffusion in Copper

Rico Rupp[†], Bart Caerts[¶], André Vantomme[¶], Jan Fransaer[#], Alexandru Vlad[*,†]*

[†]Institute of Condensed Matter and Nanosciences, UC Louvain, Place Louis Pasteur 1, B-1348 Louvain-la-Neuve, Belgium,

[¶]Institute for Nuclear and Radiation Physics, KU Leuven, Celestijnenlaan 200d, B-3001 Leuven, Belgium,

[#]Department of Materials Science, KU Leuven, Kasteelpark Arenberg 44, B-3001 Leuven, Belgium

*Corresponding author: alexandru.vlad@uclouvain.be

ABSTRACT

Copper is the conventional, broadly applied anode current collector in lithium-ion batteries, since Li does not form intermetallic alloys with Cu at room temperature. Fast diffusion and trapping of lithium in copper were however suggested in the past and the involved diffusion mechanisms are still not clarified. By using three complementary methods, we determine grain boundary and lattice diffusion of lithium in copper. We show that indiffusion into copper is not only possible from metallic lithium deposits at the surface, but also from a Li^+-containing electrolyte. Lattice diffusion (D_0 = 3.9 x 10^{-9} cm^2/s; E_a = 0.68 eV) and grain boundary diffusion (D_0 = 1.5 x 10^{-11} cm^2/s; E_a = 0.36 eV) are found to be 13 orders of magnitude lower than previously published. For practical Li-ion batteries considerations, lithium trapping in copper current collectors, which relies heavily on operating temperature and morphology, is furthermore discussed.

TOC GRAPHICS

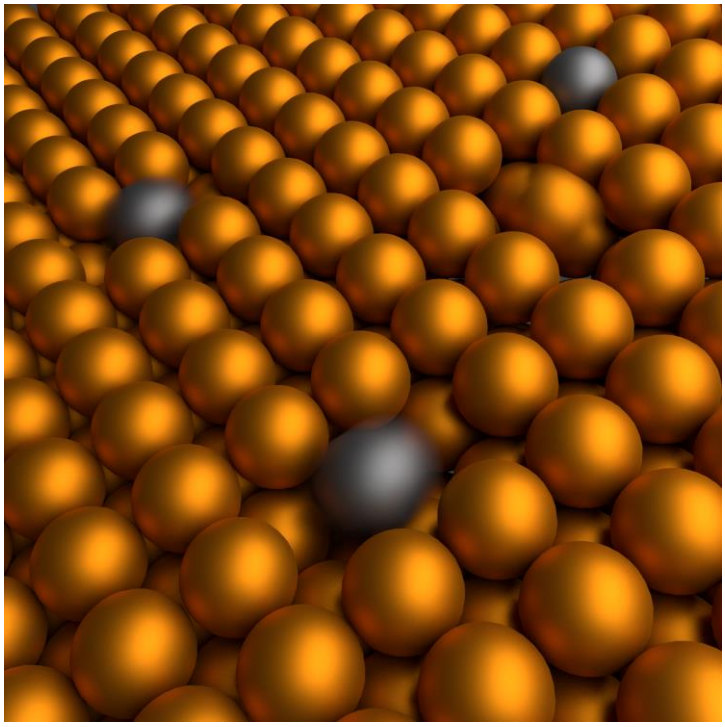

KEYWORDS

Li trapping, current collector, grain boundary, lattice, diffusion, ion-implantation, ToF-SIMS

Lithium-ion batteries (LIBs) have been commercialized as secondary cells by Sony in 1991 and the commercial use of primary lithium batteries reaches back to the 1970s with first experimental work done in the early 20th century[1]. However, many seemingly basic mechanisms involving lithium are still disputed. This includes lithium diffusion phenomena within certain components of newly developed, or even the most commonly used cells. Considering secondary LIBs, electrolytes and active electrode materials require high diffusivity of lithium-ions to ensure fast charging and discharging. Current collectors, on the other hand, are ideally inert to avoid reactions that could degrade the cells rapidly, and have no tendency to incorporate lithium(-ions) to prevent capacity loss during cycling of the cells. Whether a metal is inert with respect to lithium can generally be judged from its binary phase diagram with lithium [2]. Only a few metals are supposed not to form intermetallic alloys with lithium at room temperature, which could happen at the anode side of the battery at low potentials versus Li^+/Li. These inert metals include copper[3], nickel[4], titanium[5], magnesium[6] and iron[7].

Due to this inertness, its electrochemical stability at the required potentials, its good processability and high conductivity, copper is the common choice as current collector on the anode side. However, the generally accepted binary phase diagram also shows an apparent solubility of Li in Cu of more than 13 at.-% at room temperature[3]. While this value is open for debate, as will be discussed later, assuming its validity could lead to the assumption that Cu - even without forming intermetallic alloys - exhibits non-negligible diffusion and subsequent trapping of lithium. High diffusion rates of Li in Cu were previously reported in general[8,9], or more specifically in copper grain boundaries[10–12]. Their use as protective coatings on anode materials was therefore investigated, since protective layers with high lithium diffusivity could drastically improve the lifetime of a battery[13]. Doubts about high diffusion coefficients, however,

were expressed due to severe hindrance of the lithiation of active material if coated with a conformal copper layer with a thickness of about 100 nm or more[14–17]. These conflicting views require a quantitative determination of lithium diffusion in copper.

While the measurement of diffusion coefficients in most metals is a standard procedure [18], lithium is a special case, since it reacts with oxygen, nitrogen, or moisture in the atmosphere, makes cross-sectioning difficult due to its soft nature, and has a low melting temperature that allows rapid diffusion of other metals. To make matters even worse, very few experimental techniques exist that are able to determine Li depth profiles. To the best of our knowledge, the only direct experimental quantification of the lithium diffusion coefficient in copper was communicated by Suzuki *et al.* by using a bipolar electrochemical cell, whereby a diffusion coefficient of 10^{-7}-10^{-6} cm^2/s at room temperature was measured[11]. Gruen *et al.* estimated the diffusion coefficient on the basis of a Cu_4Li phase studied by Old and Trevena [19,20]. The experiment was performed by alloying molten lithium with copper metal at 600 °C for 12 hours. The major discrepancy is that the value of 2.6 x 10^{-7} cm^2/s for 600°C is of the same magnitude as diffusion coefficients reported by Suzuki at room temperature. Furthermore, even Gruen's values are expected to be overestimated, since interdiffusion, which is governed by the high diffusivity of Cu in liquid Li at 600 °C [21], was neglected.

Based on the inconsistencies mentioned above, we have designed and employed different techniques that are suitable to measure small diffusion coefficients at low temperatures - namely the measurement of lithium depth profiles by Time-of-Flight Secondary Ion Mass Spectrometry (ToF-SIMS) in copper metal samples after being exposed to lithium sources using three complementary protocols: (i) direct contact with metallic lithium; (ii) 0 V (vs. Li^+/Li^0) polarization in a Li-cation containing electrolyte; and (iii) high-energy ion-implantation of Li^+

into metallic copper. We were furthermore able to apply these techniques at temperatures as low as 25 °C, and to separate the effect of grain boundary diffusion and lattice diffusion.

For measurement of grain boundary diffusion coefficients, polycrystalline Cu disks with an average grain size of 11.9 ± 2.7 µm were mechanically and electrochemically polished and lithium was allowed to diffuse into the sample. While single crystals only allow diffusion through the bulk of the matrix, three types of diffusion are typically considered when studying polycrystalline samples [22]:

(i) The *A-type* diffusion stands for direct diffusion of lithium from the surface into copper through the lattice (bulk) of the sample, which is the same mechanism as in single crystals.

(ii) *B-type* diffusion describes initial fast diffusion along grain boundaries and subsequent diffusion from these defects into the bulk.

(iii) *C-type* diffusion appears when diffusion along grain boundaries is the dominating effect and in this region, it can be approximated that no lithium leaves the grain boundaries.

In the first case, metallic lithium was used as a source for indiffusion and was allowed to diffuse into copper for 11 days at temperatures between 30 °C and 120 °C (refer to SI for detailed experimental conditions). An example of the ToF-SIMS concentration depth profile of Li in a Cu polycrystal after annealing at 120 °C for 11 days is shown in Figure 1.

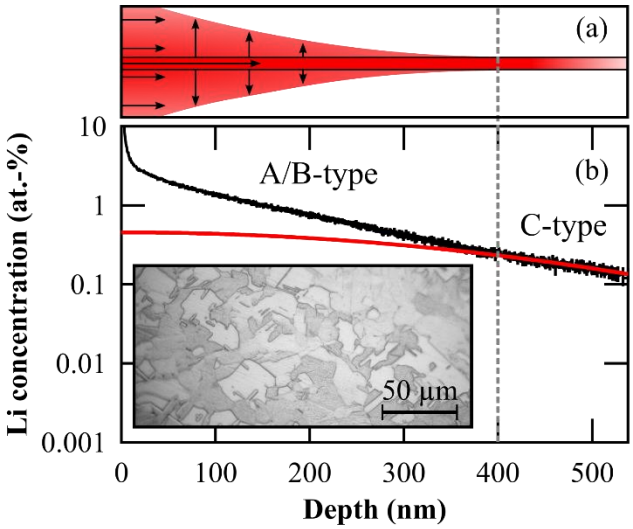

Figure 1. *(a) Schematic representation of lithium diffusion into copper along a grain boundary. (b) Exemplary ToF-SIMS Li-concentration depth profile in a Cu polycrystal after indiffusion from metallic lithium at 120 °C for 11 days (black curve), and exponential fit to the C-type region, in which grain boundary diffusion dominates (red curve). The inset shows an optical micrograph of the polycrystal surface that was etched to reveal the grain boundaries.*

Since the Cu sample in this case is polycrystalline, the Li concentration profile shows several diffusion regimes, as indicated in Figure 1b. At small depths (close to the Li/Cu interface), a mixture of A- and B-type diffusion can be observed, as schematized in Figure 1a. Diffusion in the B-type regime was described by Whipple [23], but the determination of the grain boundary diffusion coefficient in this region requires knowledge of the grain boundary width, the segregation factor of the diffusing species in the grain boundary and the bulk diffusion coefficient, and was therefore not performed here. Diffusion at higher depths is governed by C-type behavior and the logarithmic Li concentration is proportional to the square of the depth (Gaussian behavior). The concentration can be fitted by a simple Gaussian profile [24] (red curve in Figure 1b), from which the grain boundary diffusion coefficient was determined. An increased Li concentration can furthermore be observed at the surface of the Cu sample (< 10 nm) due to

minimization of the surface free energy, which has previously been observed for Cu-Li alloys [19], and due to the strong preferential reaction of lithium with oxygen or nitrogen.

In order to measure lattice diffusion coefficients, electrochemically polished Cu(100) single crystal substrates were used instead of Cu polycrystals. Since lattice diffusion in metals is typically slower than grain boundary diffusion, the annealing times were adapted depending on the respective temperature. This method, however, is limited by fast diffusion of Cu in Li at elevated temperatures[21]. The highest temperature at which reliable results were achieved was 160 °C. At higher temperatures, the Li-Cu interface becomes extremely rough due to interdiffusion, up to the point of severe dissolution of Cu into liquid Li at 250 °C. A typical ToF-SIMS depth profile after annealing at 120 °C for 28 days is shown in Figure 2.

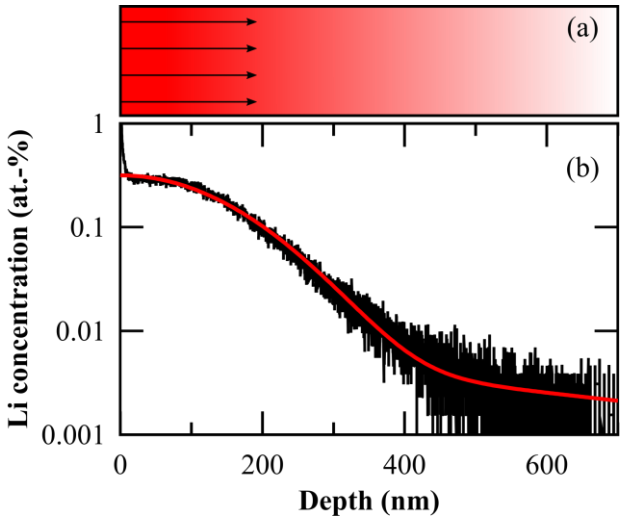

Figure 2. *(a) Schematic representation of lithium (bulk) diffusion into a copper single crystal. (b) ToF-SIMS depth profile of Li in a Cu single crystal after indiffusion from metallic lithium at 120 °C for 28 days (black), and exponential fit with tail (red).*

The boundary conditions in this particular case could be altered by a surface hold-up of lithium due to a thin oxide layer or limited solubility in copper [18] and were difficult to determine. The

measured profiles excluding the above-mentioned increased surface concentration are best described by a Gaussian function [18,25], where C is the lithium concentration, C_0 a constant related to the concentration at the boundary, t the diffusion time at a given temperature, D_l the lattice diffusion coefficient, and x the penetration depth :

$$C(x) = \frac{C_0}{\sqrt{2\pi D_l t}} \exp\left(-\frac{x^2}{4D_l t}\right) + A \exp\left(-Bx^{6/5}\right)$$

The second term including the constants A and B is added to account for the tail in the concentration profile. This tail can result from surface irregularities of the copper sample or fast diffusion paths along dislocations, which are both covered by addition of the exponential term and do not influence the calculated diffusion coefficient, as was discussed by Neumann and Lam.

Due to the temperature restrictions of the above described method - fast Cu diffusion in Li - peak broadening of ion-implanted lithium in Cu single crystals (<100>; Alineason Materials Technology) was used to analyze the lattice diffusion coefficients in the temperature range of 180 °C to 300 °C. The as-implanted ToF-SIMS profile is shown in Figure 3b.

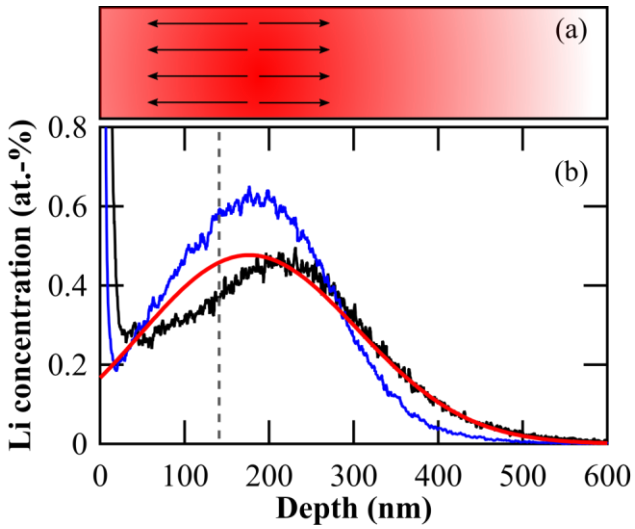

Figure 3. *(a) Schematic representation of lithium diffusion in a copper single crystal after ion-implantation. (b) ToF-SIMS depth profile after implantation (blue), after annealing at 300 °C for*

90 minutes (black), and weighted fit of the annealed profile (red). The dashed line marks the position of maximal induced vacancy concentration (refer to figure S2 for details).

Apart from the increased surface concentration of Li, which is also visible for this method, the as-implanted profile follows the expected truncated Gaussian and the profiles after annealing were analyzed using an analytical approach to peak broadening according to Malherbe et al. [26]. While the profiles after annealing show the expected peak broadening due to diffusion (see Figure 3b), a clear deviation of the profile from the expected shape is apparent. This is a result of the increased diffusion in the region around 140 nm, where ion-implantation resulted in the highest number of induced vacancies (refer to Figure S2). This effect is the so-called transient enhanced diffusion (TED). Especially the lithium concentration towards the surface is apparently increased due to TED. In order to avoid artifacts from induced vacancies and from the increased surface concentration, Malherbe's analytical equation was only fitted to the right side of the profile (high depth of penetration), where a small concentration of induced vacancies is expected (based on the modelled amount of induced vacancies, Figure S2).

Finally, the indiffusion from a Li^+-containing ionic liquid was also tested, since this setup is closer to the reality in Li-ion batteries: graphite anodes operate at potentials close to 0 V (vs. Li^+/Li^0) and occasional Li plating may occur under fast charge conditions, as well as under-potential deposition. Different cells were short-circuited (no induced Li plating), while being maintained at different temperatures (details on the setup are given in the supporting information). Since a low potential vs. Li^+/Li increases the concentration of Li^+ at the Cu surface, a larger amount of Li is expected within the Cu sample than at open circuit conditions. The inverse was done by Gąsior *et al.*, who measured the potential of Cu-Li alloys at high temperatures in molten salt electrolytes as a function of the Li-concentration in the alloy [27].

Limited by the thermal stability of the utilized ionic liquid, this method was applied only up to 100 °C. Analysis by ToF-SIMS shows that the Li-concentration depth profiles after indiffusion from Li-cation containing electrolyte show the same behavior as when in contact with Li-metal (see Figure S1), meaning that lithium can diffuse into Cu current collectors, even if no Li-metal is deposited on the surface of Cu. While the exact mechanism for Li indiffusion for this specific set of experiments is not yet clear, we presume that lithium can diffuse into Cu without the transfer of electrons across the electrolyte/Cu interface, similar to the process that Gileadi proposed for metal deposition [28,29]. Since the ionizability of Li is larger than that of Cu (the first ionization energies are 519 kJ/mol and 745 kJ/mol respectively), lithium is present as Li^+ in copper (comparable to Na in Li as described by Ott [30]). The electrons that are necessary for charge neutrality are located at the top of the Fermi level of Cu and the charge of the Li^+ impurities is shielded by local changes in electron density. This is equivalent to the metal deposition process described by Gileadi, and the fact that lithium was able to diffuse into copper without any applied current supports his claims, which remains controversial.

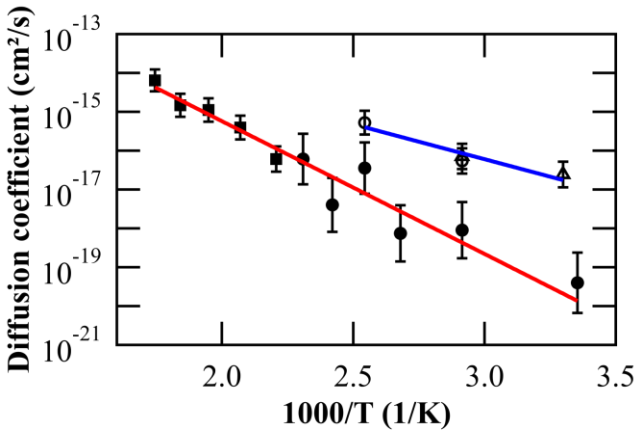

Figure 4. *Arrhenius plots of lattice diffusion coefficients from single-crystal measurements (filled symbols, red fit) and grain boundary diffusion coefficients from polycrystal measurements (hollow symbols, blue fit). The data include peak broadening of ion-implanted lithium (squares),*

indiffusion from lithium metal (circles), and indiffusion from PYR13 with Cu at 0 V vs. Li^+/Li (triangles).

The grain boundary and lattice diffusion coefficients calculated from all complementary experiments performed in this work are summarized in Figure 4. Following the same trend, the lattice diffusion coefficients extracted from indiffusion and Li^+-implantation are in good agreement with each other. This additionally confirms the validity of both methods. By avoiding the influence of interdiffusion of the two metals and any eventual surface or interface effects due to roughening or oxide layers, ion-implantation leads to a smaller error. The resulting Arrhenius equations of the lattice and grain boundary diffusion are respectively given by

$$D_l = 3.9 \cdot 10^{-9} \exp\left(-\frac{0.68\ eV}{k_B T}\right) \frac{cm^2}{s}$$

and $$D_{gb} = 1.5 \cdot 10^{-11} \exp\left(-\frac{0.36\ eV}{k_B T}\right) \frac{cm^2}{s}.$$

The activation energy for lattice diffusion with 0.68 eV is in excellent agreement with the value of 0.67 eV for the vacancy diffusion mechanism obtained by Xiong *et al.* using ab-initio calculations [31]. We did not observe a curvature of the Arrhenius plot due to divacancies at temperatures below 300 °C, which could however be related to the inherently low accuracy of the indiffusion experiments. The lower activation energy of 0.36 eV that was measured for grain boundary diffusion results from the high defect density between grains. The room temperature diffusion coefficients from Arrhenius fits are 1.3 x 10^{-20} cm²/s and 1.4 x 10^{-17} cm²/s for lattice and grain boundary diffusion, respectively. These are 13 orders of magnitude lower than previously reported values of 10^{-7}-10^{-6} cm^2/s [11].

While the diffusion coefficients provide information about the speed of Li uptake in Cu, the actual amount of Li that can potentially be trapped in current collectors cannot be obtained from

these values. The amount of Li that diffused into Cu can nevertheless be extracted from the indiffusion experiments by integration of the concentration profiles, including the increased surface concentration of lithium. The respective values for room temperature and 120 °C are listed in Table 1. As expected and confirmed by diffusion experiments, grain boundaries lead to a faster and higher Li uptake in copper. Even though lithium was only allowed to diffuse for 11 days into the polycrystals, while diffusion into Cu single crystals was done for 28 days, a 3 to 4 times higher mass-uptake of Li in Cu was found for the polycrystalline samples as compared to the single crystals. This gives evidence that smaller grains (and therefore more grain boundaries) lead to a larger uptake of lithium.

Table 1. *Mass of lithium that diffused into copper during the indiffusion experiments at different temperatures and durations, as extracted from ToF-SIMS depth profiles.*

Temperature	**Single crystal (28 days)**	**Polycrystal (11 days)**
27 °C (± 3 °C)	3 ng/cm²	10 ng/cm²
120 °C	156 ng/cm²	591 ng/cm²

It is worth being pointed out that the commonly accepted Cu-Li binary phase diagram is based on experiments that were conducted by Klemm *et al.* by using fine Cu powder [32]. This Cu powder offers many grain boundaries and a high surface area where Li concentration is increased, as well as an increased total amount of surface oxide with high lithium content, as compared to bulk samples with a low surface-to-volume ratio. We believe thus that the actual bulk solubility of Li in Cu is much lower than shown in the binary phase diagram.

The polycrystals utilized here were hot-rolled and have thus a relatively large average grain size of 11.9 µm. Battery current collectors, on the other hand, are typically electrodeposited and have average grain sizes closer to 1 µm. We expect this to be the reason for the much larger amount of 10.6 µg/cm² lithium that was found by Rehnlund *et al.* after 7 days at 50 °C (lithium in direct contact with copper) [8]. Whether the amount of trapping Li in Cu could be neglected or not, will strongly depend on the chemistry and configuration of the anode electrodes used, as well as operation temperature. When using low mass loading in thin film anodes, for example, lithium trapping might be found to lead to significant relative losses, especially when long lifetimes at elevated temperatures are aspired. Room-temperature operation, even for a typical battery lifetime, is expected to lead to minimal Li losses in typically used anodes. As was previously proposed by Lv *et al.* [10] and is confirmed here, the use of copper current collectors with a large grain size could be a valid method to limit lithium losses when necessary.

ASSOCIATED CONTENT

Supporting Information Available: ToF-SIMS measurements and determination of relative sensitivity factors; bipolar cells for diffusion measurements and discussion of literature on Li diffusion in Cu; indiffusion from metallic lithium and electrolytes; Ion-implantation and the influence of induced vacancies on peak-broadening. (PDF)

AUTHOR INFORMATION

The authors declare no competing financial interests.

ACKNOWLEDGMENT

Rico Rupp is a Research Fellow at the Belgian *Fonds de la Recherche Scientific* (F.R.S-FNRS). This work was supported by the FNRS - U.N011.18 - DEMIST, CF-ARC (18/23-093) MICROBAT, Fund for Scientific Research-Flanders, the KU Leuven BOF and the EU Horizon 2020 program (No824096 - RADIATE).

REFERENCES

(1) van Schalkwijk, W. A.; Scrosati, B. *Advances in Lithium-Ion Batteries*; van Schalkwijk, W. A., Scrosati, B., Eds.; Springer US: Boston, MA, 2002.

(2) Gottstein, G. *Physikalische Grundlagen der Materialkunde*, 3rd edition; Springer-Verlag: Berlin, Heidelberg, 2007.

(3) Okamoto, H. Cu-Li (Copper-Lithium). *J. Phase Equilibria Diffus.* **2011**, *32* (2), 172–172.

(4) Predel, B. Li-Ni (Lithium-Nickel). In *Li-Mg – Nd-Zr. Landolt-Börnstein - Group IV Physical Chemistry (Numerical Data and Functional Relationships in Science and Technology)*; Madelung, O., Ed.; Springer: Berlin, Heidelberg, 1990; Vol. 5H, p 1.

(5) Bale, C. W. The Li-Ti (Lithium-Titanium) System. *Bull. Alloy Phase Diagrams* **1989**, *10*

(2), 135–138.

(6) Nayeb-Hashemi, A. A.; Clark, J. B.; Pelton, A. D. The Li-Mg (Lithium-Magnesium) System. *Bull. Alloy Phase Diagrams* **1984**, *5* (4), 365–374.

(7) Predel, B. Fe-Li (Iron-Lithium). In *Dy-Er – Fr-Mo. Landolt-Börnstein - Group IV Physical Chemistry (Numerical Data and Functional Relationships in Science and Technology)*; Madelung, O., Ed.; Springer Berlin Heidelberg: Berlin, Heidelberg, 1995; pp 1–3.

(8) Rehnlund, D.; Lindgren, F.; Böhme, S.; Nordh, T.; Zou, Y.; Pettersson, J.; Bexell, U.; Boman, M.; Edström, K.; Nyholm, L.; et al. Lithium Trapping in Alloy Forming Electrodes and Current Collectors for Lithium Based Batteries. *Energy Environ. Sci.* **2017**, *10*, 1350–1357.

(9) Rehnlund, D.; Pettersson, J.; Edström, K.; Nyholm, L. Lithium Trapping in Microbatteries Based on Lithium- and Cu 2 O-Coated Copper Nanorods. *ChemistrySelect* **2018**, *3* (8), 2311–2314.

(10) Lv, S.; Verhallen, T.; Vasileiadis, A.; Ooms, F.; Xu, Y.; Li, Z.; Li, Z.; Wagemaker, M. Operando Monitoring the Lithium Spatial Distribution of Lithium Metal Anodes. *Nat. Commun.* **2018**, *9* (1), 2152–2163.

(11) Suszuki, J.; Sekine, K.; Takamura, T. Measurements of Li Diffusion Rate in Metal Using a Bipolar Cell in Which a Tungsten Electrode Is Used to Sense Li^+ Ion Concentration. *Electrochemistry* **2003**, *71* (12), 1120–1122.

(12) Neudecker, B. J.; Dudney, N. J.; Bates, J. B. "Lithium-Free" Thin-Film Battery with In Situ Plated Li Anode. *J. Electrochem. Soc.* **2000**, *147* (2), 517.

(13) Vlad, A.; Rupp, R. Coated Silicon Nanowires for Battery Applications. In *Silicon Nanomaterials Sourcebook - Volume I*; Sattler, K. D., Ed.; Taylor & Francis Group: Boca Raton, 2017; pp 475–494.

(14) Vlad, A.; Reddy, A. L. M.; Ajayan, A.; Singh, N.; Gohy, J.-F.; Melinte, S.; Ajayan, P. M.

Roll up Nanowire Battery from Silicon Chips. *Proc. Natl. Acad. Sci. U. S. A.* **2012**, *109* (38), 15168–15173.

(15) McDowell, M. T.; Lee, S. W.; Wang, C.; Cui, Y. The Effect of Metallic Coatings and Crystallinity on the Volume Expansion of Silicon during Electrochemical Lithiation/Delithiation. *Nano Energy* **2012**, *1* (3), 401–410.

(16) Sethuraman, V. A.; Kowolik, K.; Srinivasan, V. Increased Cycling Efficiency and Rate Capability of Copper-Coated Silicon Anodes in Lithium-Ion Batteries. *J. Power Sources* **2011**, *196* (1), 393–398.

(17) Sandu, G.; Brassart, L.; Gohy, J. F.; Pardoen, T.; Melinte, S.; Vlad, A. Surface Coating Mediated Swelling and Fracture of Silicon Nanowires during Lithiation. *ACS Nano* **2014**, *8* (9), 9427–9436.

(18) Neumann, G.; Tuijn, C. *Self-Diffusion and Impurity Diffusion in Pure Metals*, 1st edition; Elsevier, 2008.

(19) Gruen, D. M.; Krauss, A. R.; Susman, S.; Venugopalan, M.; Ron, M. Gibbsian and Radiation-induced Segregation in Cu–Li and Al–Li Alloys. *J. Vac. Sci. Technol. A Vacuum, Surfaces, Film.* **1983**, *1* (2), 924–928.

(20) Old, C. F.; Trevena, P. Reaction in Copper-Lithium System and Its Implications for Liquid-Metal Embrittlement. *Met. Sci.* **1981**, *15* (7), 281–285.

(21) Ott, A. Interstitial-Like Diffusion of Copper in Lithium. *J. Appl. Phys.* **1969**, *40* (6), 2395–2396.

(22) Kaur, I.; Gust, W. Grain and Interphase Boundary Diffusion. In *Diffusion in solid metals and alloys*; Mehrer, H., Ed.; Springer-Verlag: Berlin, 1990; pp 630–716.

(23) Whipple, R. T. P. CXXXVIII. Concentration Contours in Grain Boundary Diffusion. *London, Edinburgh, Dublin Philos. Mag. J. Sci.* **1954**, *45* (371), 1225–1236.

(24) Crank, J. *The Mathematics of Diffusion*, 2nd edition; Clarendon press: Oxford, 1975.

(25) Lam, N. Q.; Rothman, S. J.; Mehrer, H.; Nowicki, L. J. Self-diffusion in Silver at Low Temperatures. *Phys. Status Solidi* **1973**, *57* (1), 225–236.

(26) Malherbe, J. B.; Selyshchev, P. A.; Odutemowo, O. S.; Theron, C. C.; Njoroge, E. G.; Langa, D. F.; Hlatshwayo, T. T. Diffusion of a Mono-Energetic Implanted Species with a Gaussian Profile. *Nucl. Instruments Methods Phys. Res. Sect. B Beam Interact. with Mater. Atoms* **2017**, *406*, 708–713.

(27) Gasior, W.; Onderka, B.; Moser, Z.; Debski, A.; Gancarz, T. Thermodynamic Evaluation of Cu-Li Phase Diagram from EMF Measurements and DTA Study. *Calphad Comput. Coupling Phase Diagrams Thermochem.* **2009**, *33* (1), 215–220.

(28) Gileadi, E. Can an Electrode Reaction Occur without Electron Transfer across the Metal/Solution Interface? *Chem. Phys. Lett.* **2004**, *393* (4–6), 421–424.

(29) Gileadi, E. The Enigma of Metal Deposition. *J. Electroanal. Chem.* **2011**, *660* (2), 247–253.

(30) Ott, A. Impurity Diffusion in Lithium. *Zeitschrift für Naturforsch.* **1970**, *25 a*, 1477–1483.

(31) Xiong, Z.; Shi, S.; Ouyang, C.; Lei, M.; Hu, L.; Ji, Y.; Wang, Z.; Chen, L. Ab Initio Investigation of the Surface Properties of Cu(111) and Li Diffusion in Cu Thin Film. *Phys. Lett. Sect. A Gen. At. Solid State Phys.* **2005**, *337* (3), 247–255.

(32) Klemm, W.; Volavsek, B. Zur Kenntnis Des Systems Lithium-Kupfer. *ZAAC - J. Inorg. Gen. Chem.* **1958**, *296* (1–6), 184–187.